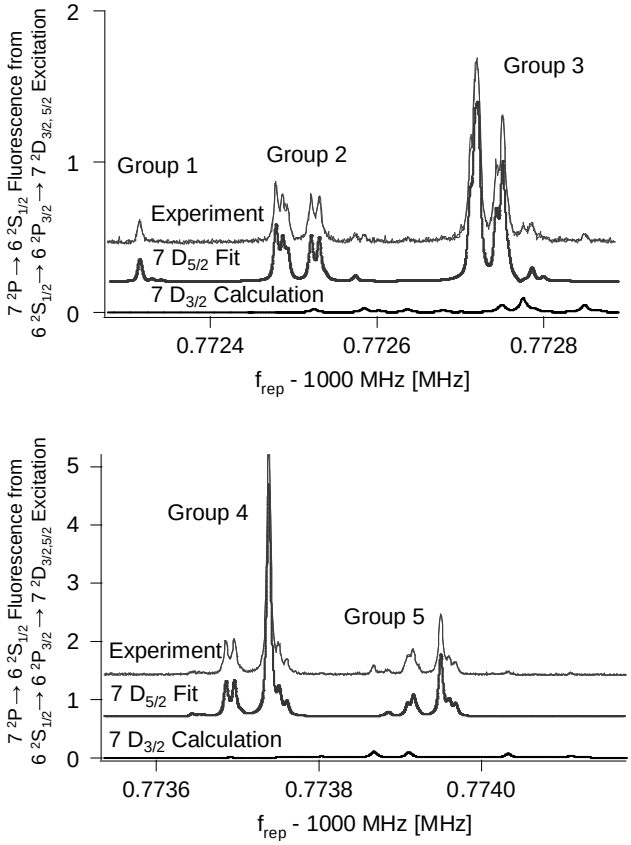

FIG. 13: The experimental spectrum (upper trace), fit to the $6S_{1/2} \rightarrow 6P_{3/2} \rightarrow 7D_{5/2}$ transition (middle trace), and of the calculated contribution from the $6S_{1/2} \rightarrow 6P_{3/2} \rightarrow 7D_{3/2}$ transition (lower trace). Note that the vertical scales are different for the two figures.

transition. For the first stage the intensity over the 10 nm bandwidth was varied from $\approx 22\,\mathrm{W/cm^2}$ to $\approx 5\,\mathrm{W/cm^2}$. Data were taken at cell temperatures corresponding to saturated vapor pressures of 0.15, 1.05, 3.9, and 8.5 mPa. The dependence of the center-of-gravity on the varied parameters is shown in Fig. 14 and are summarized in Table I.

As with the previous transitions there was no significant shift arising from the light power. A linear fit gave a slope of $-23(62)$ kHz$/P$, where P is the normalized operating power. This gives us an uncertainty of 85 kHz in the center-of-gravity frequency. We found uncertainties in the hyperfine A and B constants of 11 kHz and 458 kHz, respectively.

Unlike the other transitions studied here, we did observe a dependence of the center-of-gravity on the magnetic field (Fig. 14). There was clear evidence of broadening in the peaks at the largest magnetic fields. We attribute the shift to a break down of the line-shape model as the line broadens coupled with the overlap of the peaks. In this case, we base our estimate of the uncertainty on the difference of the point taken at the zeroed field with the residual field and find an uncertainty of

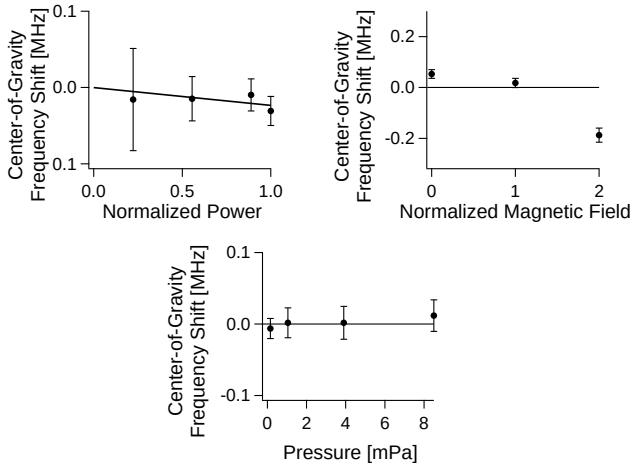

FIG. 14: The dependence of the center-of-gravity frequencies for the $6S_{1/2} \rightarrow 6P_{3/2} \rightarrow 7D_{5/2}$ transition on the power (upper left), the magnetic field (upper right), and the Cs vapor pressure (bottom). The straight line in the power dependence plot is a linear weighted fit to the data. The vertical axis has been offset and centered so that the nominal operating point is at zero. The power is plotted as a function of the fraction of the maximum power. The magnetic field is plotted as a function of the residual magnetic field.

35 kHz in the optical frequency. There is no evidence for a dependence of the extracted hyperfine A constant, and we find a magnetic-field uncertainty of 6 kHz for it. For the B constant we find an uncertainty of 125 kHz.

We see no clear evidence for any temperature dependent effects. Using the larger of standard deviation or the uncertainty in the mean, we find uncertainties of 7 kHz, 1 kHz, and 38 kHz for the temperature-dependent uncertainties of the center-of-gravity frequency, the hyperfine A constant, and the hyperfine B constant, respectively

Applying these uncertainties we find

$$\begin{aligned} \nu_{6S_{1/2}:7D_{5/2}} &= 781\,522\,153.68(16)\,\mathrm{MHz} \\ A_{7D_{5/2}} &= -1.717(15)\,\mathrm{MHz} \\ B_{7D_{5/2}} &= -0.18(52)\,\mathrm{MHz}. \end{aligned}$$

V. CONCLUSIONS

We have used the technique of velocity-selective two-photon excitation to measure the center-of-gravity frequencies and the hyperfine coupling constants for the $8S_{1/2}$, $9S_{1/2}$, $7D_{3/2}$, and $7D_{5/2}$ states of Cs. The results for all of the transitions are summarized and compared to other published experimental values in Table II. This technique has potential metrological applications for secondary frequency standards at optical wavelengths. At a more fundamental level, the hyperfine coupling measurements are valuable in improving atomic structure calculations. The measurement accuracy of multiple transitions at significantly different wavelengths rivals that of